高压物理学报
CHINESE JOURNAL OF HIGH PRESSURE PHYSICS

第 32 卷 第 1 期
2018 年 2 月

高 压 物 理 学 报
CHINESE JOURNAL OF HIGH PRESSURE PHYSICS

Vol. 32, No. 1
Feb., 2018

DOI: 10.11858/gywlxb.20170532

Influence of Specimen Size in SHPB Tests on Concrete*

ZHAO Fuqi, XU Peibao, WEN Heming

(*CAS Key Laboratory for Mechanical Behavior and Design of Materials, University of Science and Technology of China, Hefei* 230027, *China*)

Abstract: The split Hopkinson pressure bar (SHPB) tests are often conducted to obtain the dynamic compressive strengths of concrete-like materials which need to be interpreted or analyzed correctly as these data are very important for the construction of reliable constitutive equations used in numerical simulations. In the present work, a numerical study is performed on the influence of specimen size on concrete in SHPB tests using a rate-independent material model. A new empirical equation for the dynamic increase factor due to inertia (confinement) effect is also proposed which took account of specimen size effect through its volume. It is shown that the empirical formula agrees well with the numerical results for the SHPB tests on concrete with different specimen sizes, and the dynamic increase factor due to inertia (confinement) effect increases with the increase of specimen size.

Keywords: SHPB test; concrete; inertia (confinement) effect; specimen size effect; numerical simulation

CLC number: O347.3 **Document code**: A

Dynamic compressive strengths of concrete-like materials are usually obtained by conducting laboratory tests such as split Hopkinson pressure bar (SHPB) tests[1-5]. Many empirical formulae for dynamic increase factor (DIF) based on laboratory test data were reported in the related literature Ref. [6-9].

It has to be mentioned here that the SHPB test data available for concrete materials in the literature were very scattered[7-10] due to the combined effects of strain rate, inertia and specimen size. More comprehensive investigation and discussion of the possible influencing factors can be also obtained in Ref. [1,2,7-11]. The inertia (confinement) effect has been widely investigated experimentally[12], theoretically[13-14], numerically[5,15] and an empirical equation for the dynamic increase factor due to inertia (confinement) effect was suggested in Ref. [16], which took no account of the effect of concrete specimen size. As strain rate effects on the compressive strengths of concrete-like materials play an important part in the construction of material constitutive models which, in turn, exert a great deal of influence on the numerical simulations of concrete structures subjected to intense dynamic loadings, it is, therefore necessary to obtain the pure strain rate effect data by eliminating the data due to the effects of inertia (confinement) and specimen size from SHPB tests.

* **Received date**: 2017-01-16; **Revised date**: 2017-03-24

Foundation item: National Natural Science Foundation of China (11572317)

Biography: ZHAO Fuqi (1989—), male, doctoral student, major in impact dynamics.
E-mail: zfq126@mail.ustc.edu.cn

Corresponding author: WEN Heming (1965—), male, Ph. D, professor, major in impact dynamics.
E-mail: hmwen@ustc.edu.cn

© 2018 Institute of Fluid Physics, China Academy of Engineering Physics

In the present study, numerical simulations with a rate-independent material model are carried out on the influence of specimen size in SHPB tests on concrete and a new empirical equation for the dynamic increase factors due to inertia (confinement) effect is proposed which takes account of specimen size effect through its volume. Comparisons are made between the results from the numerical simulation and those from the new empirical formula and discussed.

1 Material Model

The computational constitutive model for concrete developed in Ref. [1] is used to simulate the SHPB tests on concrete in the present study. This material model consists of equation of state (EOS), strength model including Lode effect, damage criteria and strain rate effects, etc.

1.1 Equation of State

The porous equation of state is used in the present study and can be expressed as[17]

$$\bar{\mu}=\frac{\rho\alpha}{\rho_0\alpha_0}-1=\frac{\alpha}{\alpha_0}(1+\mu)-1 \tag{1}$$

where $\mu=\rho/\rho_0-1$ is the volumetric strain, in which ρ and ρ_0 are respectively the current and initial densities; $\alpha=\rho_s/\rho$ and $\alpha_0=\rho_{s0}/\rho_0$ are the current and initial porosities in which ρ_s and ρ_{s0} are the current and initial densities of solid (fully-compacted) material.

For $\bar{\mu}>0$, concrete material is under compression condition

$$\begin{cases}\alpha=\max\left\{1,\min\left[\alpha_0,1+(\alpha_0-1)\left(\dfrac{p_{\text{lock}}-p}{p_{\text{lock}}-p_{\text{crush}}}\right)^n\right]\right\}\\ p=K_1\bar{\mu}+K_2\bar{\mu}^2+K_3\bar{\mu}^3\end{cases} \tag{2}$$

where K_1, K_2 and K_3 are the bulk moduli for fully compacted concrete material, p_{crush} is the pressure at which pore collapse occurs, p_{lock} is the pressure beyond which concrete material is fully compacted, n is the compaction exponent.

For $\bar{\mu}<0$, concrete material is under tension condition. Hence, the pressure is

$$p=K_1\bar{\mu} \tag{3}$$

1.2 Strength Model

The strength surface of concrete can be written in the following form[1]

$$Y=\begin{cases}3(p+f_{\text{tt}})r(\theta,e) & p\leqslant 0\\ \left[3f_{\text{tt}}+\dfrac{3p(f_{\text{cc}}-3f_{\text{tt}})}{f_{\text{cc}}}\right]r(\theta,e) & 0<p<\dfrac{f_{\text{cc}}}{3}\\ \left[f_{\text{cc}}+Bf'_{\text{c}}\left(\dfrac{p}{f'_{\text{c}}}-\dfrac{f_{\text{cc}}}{3f'_{\text{c}}}\right)^N\right]r(\theta,e) & p\geqslant\dfrac{f_{\text{cc}}}{3}\end{cases} \tag{4}$$

where $f_{\text{cc}}=f'_{\text{c}}\delta_{\text{m_t}}\eta_{\text{c}}$ and $f_{\text{tt}}=f_{\text{t}}\delta_{\text{t}}\eta_{\text{t}}$ in which f'_{c} and f_{t} are the static compressive and tensile strength, $\delta_{\text{m_t}}$ and δ_{t}[2] are the dynamic increase factors due to strain rate effects only in compression and tension, η_{c} and η_{t}[18-20] are shape functions which represent shear damage and tensile softening of concrete respectively; B and N are empirical constants; $r(\theta,e)$[21] is the Lode effect with θ and e being the Lode angle, the ratio of the tensile meridian to the compression meridian, respectively.

By setting $f_{\text{tt}}=0$ and $f_{\text{cc}}=f'_{\text{c}}r$ (residual strength), the residual strength surface for concrete can be obtained from Eq. (4)

$$Y=\begin{cases}3pr(\theta,e) & 0<p<\dfrac{f'_{\text{c}}r}{3}\\ \left[f'_{\text{c}}r+Bf'_{\text{c}}\left(\dfrac{p}{f'_{\text{c}}}-\dfrac{r}{3}\right)^N\right]r(\theta,e) & p\geqslant\dfrac{f'_{\text{c}}r}{3}\end{cases} \tag{5}$$

Other information about shear, tensile damage, Lode effect and strain rate effect can be found in Ref. [1-2].

2 Specimen Size Effect

In this section, the commercial software LS-DYNA3D with user-defined subroutines is used to carry out the numerical study on the influence of specimen size in SHPB tests on concrete using a recently developed constitutive model for concrete[1] by setting the material DIF (δ) equal to 1. The inertia effect dynamic enhancement factor (R_c) can be obtained by dividing the strength results of simulation by quasi-static strength. The values of various parameters used in the material model are listed in Table 1[1]. In this case, the numerically obtained strength increment of the studied specimen is attributed to the inertia (confinement) effect only.

Table 1　Material parameters of concrete[1]

Parameters of EOS							
ρ_0/(kg·m^{-3})	ρ_{s0}/(kg·m^{-3})	p_{crush}/MPa	p_{lock}/GPa	n	K_1/GPa	K_2/GPa	K_3/GPa
2 400	2 680	15.2	3	3	13.9	30	10

Parameters of constitutive model														
Strength surface					Shear damage				Tensile damage			Lode effect		
f'_c/MPa	f_t/MPa	B	N	G/GPa	λ_s	l	r	λ_m	c_1	c_2	ε_{frac}	e_1	e_2	e_3
45.6	3.8	1.7	0.7	10.5	4.6	0.45	0.3	0.3	3	6.93	0.007	0.65	0.01	5

An SHPB system contains incident and transmitter pressure bars with a short specimen between them, as shown in Fig. 1. A stress pulse of trapezium shape is applied to the incident pressure bar as shown schematically in Fig. 2 in which the incident stress starts from 0, quickly rises to the peak value of p_{peak} at t_1, keeps as a constant for t_2, then drops back to 0 after t_3 and are summarized in Table 2.

Table 2　Load function parameters for direct compression analyses

t_1/μs	t_2/μs	t_3/μs	p_{peak}/MPa
25	200	25	Varies

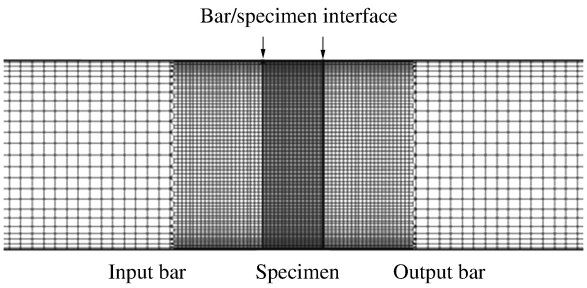

Fig. 1　Finite element model of SHPB system

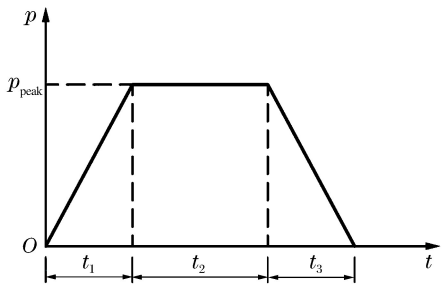

Fig. 2　Loading function used in finite element analysis

Friction is an important factor which needs to be considered. However, in SHPB tests on concrete the effect of friction is negligibly small[22] in terms of its contribution to the total dynamic increase factor and is usually ignored in numerical simulations[23]. Moreover, in SHPB tests measures are usually taken (i. e. by applying lubricant to both ends of concrete samples) to further reduce the effect of friction. Hence, in the present study the effect of friction is also ignored in the numerical simulations.

In this study, the dynamic strength increase factor is employed to reflect the effect of specimen size in SHPB tests on concrete. If there is no size effect there will be no difference for concrete samples with different sizes or volumes in terms of the dynamic increase factors at the same strain rate. Otherwise there will be size effect in SHPB tests on concrete.

Fig. 3 shows the numerical results for the dynamic increase factor due to inertia (confinement) effect R_c for concrete specimens with the same volume of different length/diameter ratios (i. e., ∅51 mm×51 mm, ∅64 mm×32 mm, ∅74 mm×24 mm) whilst Fig. 4 shows the numerical results for concrete samples with different volume of the same length/diameter ratios (i. e., ∅64 mm×32 mm, ∅80 mm×40 mm). It can be seen from Fig. 3 that the inertia effect is mainly related to the specimen volume and is insensitive to the length/diameter ratio when the volume and the material parameters of the specimens are kept the same. It also can be seen from Fig. 4 that the dynamic increase factor due to inertia (confinement) effect increases with the increase of the concrete specimen volume, which indicates that size effect does exist in SHPB tests on concrete as described above.

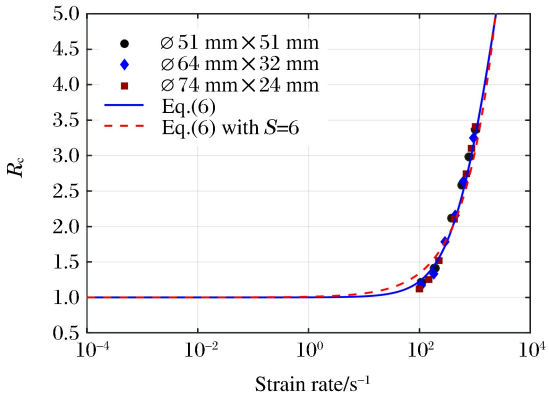

Fig. 3　Comparison of Eq. (6) with numerical results for dynamic increase factor due to inertia (confinement) effect for concrete specimens with the same volume of different length/diameter ratios

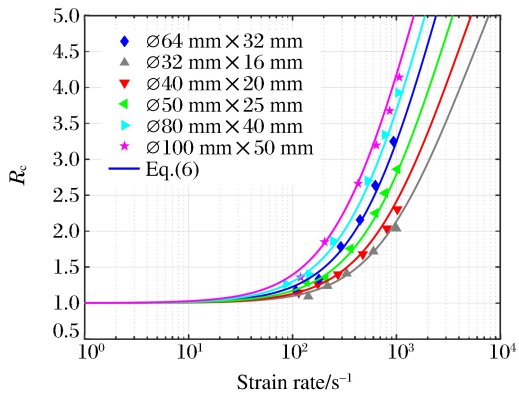

Fig. 4　Comparison of Eq. (6) with numerical results for dynamic increase factor due to inertia (confinement) effect for concrete specimens with different volume of the same length/diameter ratio

3　A New Empirical Equation

On the basis of the numerical results discussed in the previous section, a new empirical equation which takes consideration of the specimen size effect in SHPB tests on concrete is suggested here to describe the dynamic increase factor due to inertia (confinement) effect R_c by using the monotonically increasing and continuous properties of exponential functions in a simple and easy to use form, namely

$$R_c = S^{\lg\left(\frac{\dot{\varepsilon}}{\dot{\varepsilon}_0}\right) + \frac{1}{\beta}\lg\left(\frac{V}{V_0}\right)^{-W}} + 1 \tag{6}$$

where S, W, β are the constants to be determined numerically, $\dot{\varepsilon}$ is the strain rate, $\dot{\varepsilon}_0$ is the reference strain rate for a reference specimen usually taken to be $\dot{\varepsilon}_0 = 1.0\ \mathrm{s}^{-1}$, V is the volume of a concrete specimen under investigation, V_0 is the volume of a concrete sample with a reference size, say, ∅51 mm×51 mm. Set $V = V_0$ in Eq. (6), one obtains the dynamic increase factor due to inertia effect for the reference concrete specimen R_{c0}.

In the following, first, one determines the values of S and W in Eq. (6) using the numerical results for the concrete specimen with the same volume (i. e. $V = V_0$) as presented in Fig. 3 and, then, the value of β in Eq. (6) using the numerical results for the concrete samples with different sizes/volumes as given in Fig. 4.

Fig. 3 shows the comparison between the numerical results and Eq. (6) with $S=6$, $W=2.8$ and $V=V_0$ as indicated by the dashed line. It can be seen from Fig. 3 that reasonable agreement is obtained. Further examination reveals that the value of S in Eq. (6) should not be a constant but a function of strain rate. The slope of the curve is too small at the low strain rate, and too large at the high strain rate. By using the centrosymmetric properties of the hyperbolic tangent and the x-axis paralleled, S is taken as the following form to increase the slope of the curve at the low strain rate and decrease the slope at the high strain rate, namely

$$S=-F_i \tanh\left[\lg\left(\frac{\dot{\varepsilon}}{\dot{\varepsilon}_0}-W_i\right)S_i\right]+G_i \tag{7}$$

where F_i, W_i, S_i, G_i are the constants determined using the numerical results for concrete samples with constant volume as presented in Fig. 3, namely, $F_i=6.0$, $W_i=2.8$, $S_i=0.8$, $G_i=8.5$. The solid line in Fig. 3 is predicted from Eq. (6) with $V=V_0$ together with Eq. (7). It is clear from Fig. 3 that good agreement is obtained.

Fig. 4 shows the comparison between Eq. (6) with $\beta=2.7$ and the numerical results obtained for the concrete samples with different sizes/volumes. The values of all the other parameters in Eq. (6) are listed in Table 3. It is evident from Fig. 4 that the present model agrees well with the numerical simulations.

Table 3　Values of various parameters in Eq. (6) and Eq. (7)

$\dot{\varepsilon}_0/\mathrm{s}^{-1}$	F_i	S_i	W_i	G_i	W	β
1.0	6.0	0.8	2.8	8.5	2.8	2.7

In order to verify the validity of Eq. (6) more numerical simulations are performed on concrete specimens with different sizes. The numerical results are also presented in Fig. 4 and comparisons are also made between Eq. (6) and the numerical results. It can be seen from Fig. 4 that good agreement is obtained.

Fig. 5 shows the normalization of all the numerical results for concrete specimens with different sizes as given in Fig. 3 and Fig. 4 with respect to those for the reference concrete sample, namely, ∅51 mm×51 mm. It is clear from Fig. 5 that all the numerical results collapse into one line. It lends further support to the validity of Eq. (6) for the dynamic increase factor due to inertia (confinement) effect which takes into consideration the influence of specimen size.

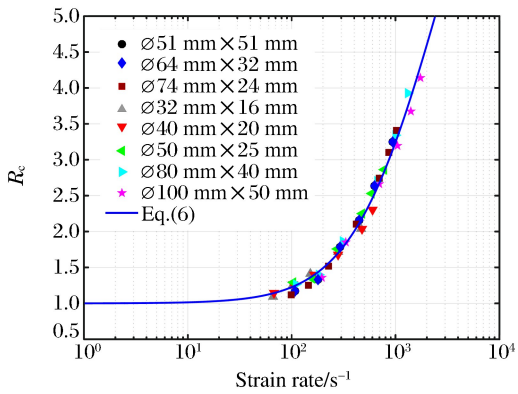

Fig. 5　Variation of normalized numerically obtained dynamic increase factor due to inertia (confinement) effect with strain rate

4　Conclusions

The influence of specimen size in SHPB tests on concrete has been investigated numerically using a rate-independent material model. A new empirical equation for the dynamic increase factor due to inertia (confinement) effect has also been proposed which takes into account the specimen size effect through its volume. It is demonstrated that the new empirical formula agrees well with the numerical results for SHPB tests on concrete with different specimen sizes.

References:

[1] XU H, WEN H M. A computational constitutive model for concrete subjected to dynamic loadings [J]. International Journal of Impact Engineering, 2016, 91: 116-125.

[2] XU H, WEN H M. Semi-empirical equations for the dynamic strength enhancement of concrete-like materials [J]. International Journal of Impact Engineering, 2013, 60: 76-81.

[3] TEDESCO J W, HUGHES M L, ROSS C A. Numerical simulation of high strain rate concrete compression tests [J]. Computers & Structures, 1994, 51(1): 65-77.

[4] GROTE D L, PARK S W, ZHOU M. Dynamic behavior of concrete at high strain rates and pressures: Ⅰ. experimental characterization [J]. International Journal of Impact Engineering, 2001, 25(9): 869-886.

[5] LI Q M, LU Y B, MENG H. Further investigation on the dynamic compressive strength enhancement of concrete-like materials based on split Hopkinson pressure bar tests. Part Ⅱ: numerical simulations [J]. International Journal of Impact Engineering, 2009, 36(12): 1335-1345.

[6] HAO H, TARASOV B G. Experimental study of dynamic material properties of clay brick and mortar at different strain rates [J]. Australian Journal of Structural Engineering, 2008, 8(2): 117-132.

[7] BISCHOFF P H, PERRY S H. Compressive behaviour of concrete at high strain rates [J]. Materials & Structures, 1991, 24(6): 425-450.

[8] TEDESCO J W, ROSS C A. Strain-rate-dependent constitutive equations for concrete [J]. Journal of Pressure Vessel Technology, 1998, 120(4): 398-405.

[9] ZHOU X Q, HAO H. Mesoscale modelling and analysis of damage and fragmentation of concrete slab under contact detonation [J]. International Journal of Impact Engineering, 2009, 36(12): 1315-1326.

[10] COTSOVOS D M, PAVLOVIC M N. Numerical investigation of concrete subjected to compressive impact loading. Part 1: a fundamental explanation for the apparent strength gain at high loading rates [J]. Computers & Structures, 2008, 86(1): 145-163.

[11] HAO H, HAO Y, LI Z X. A numerical study of factors influencing high-speed impact tests of concrete material properties [C]//Proceedings of the 8th International Conference on Shock and Impact Loads on Structures. Adelaide: CI-Premier Pte Ltd, 2009: 37-52.

[12] ZHANG M, WU H J, LI Q M, et al. Further investigation on the dynamic compressive strength enhancement of concrete-like materials based on split Hopkinson pressure bar tests. Part I: experiments [J]. International Journal of Impact Engineering, 2009, 36(12): 1327-1334.

[13] FORRESTAL M J, WRIGHT T W, CHEN W. The effect of radial inertia on brittle samples during the split Hopkinson pressure bar test [J]. International Journal of Impact Engineering, 2007, 34(3): 405-411.

[14] ZHANG M, LI Q M, HUANG F L, et al. Inertia-induced radial confinement in an elastic tubular specimen subjected to axial strain acceleration [J]. International Journal of Impact Engineering, 2010, 37(4): 459-464.

[15] HAO Y, HAO H, LI Z X. Numerical analysis of lateral inertial confinement effects on impact test of concrete compressive material properties [J]. International Journal of Protective Structures, 2010, 1: 145-168.

[16] LI Q M, MENG H. About the dynamic strength enhancement of concrete-like materials in a split Hopkinson pressure bar test [J]. International Journal of Solids and Structures, 2003, 40(2): 343-360.

[17] HERRMANN W. Constitutive equation for the dynamic compaction of ductile porous materials [J]. Journal of Applied Physics, 1969, 40(6): 2490-2499.

[18] HORDIJK D A. Local approach to fatigue of concrete [D]. Delft: Delft University of Technology, 1991.

[19] MALVAR L J, CRAWFORD J E, WESEVICH J W, et al. A plasticity concrete material model for DYNA3D [J]. International Journal of Impact Engineering, 1997, 19(9): 847-873.

[20] HARTMANN T, PIETZSCH A, GEBBEKEN N. A hydrocode material model for concrete [J]. International Journal of Protective Structures, 2010, 1(4): 443-468.

[21] WILLAM K J, WARNKE E P. Constitutive model for the triaxial behavior of concrete [J]. Proceedings of International Association for Bridge and Structural Engineering, 1975, 19(1): 1-30.

[22] HAO Y, HAO H, LI Z X. Influence of end friction confinement on impact tests of concrete material at high strain rate [J]. International Journal of Impact Engineering, 2013, 60: 82-106.

[23] LI Q M, LU Y B, MENG H. Further investigation on the dynamic compressive strength enhancement of concrete-like materials based on split Hopkinson pressure bar tests. Part Ⅱ: numerical simulations [J]. International Journal of Impact Engineering, 2009, 36(12): 1335-1345.

SHPB 混凝土实验中试件尺寸的影响

赵福祺，徐沛保，文鹤鸣

（中国科学技术大学，中科院材料力学行为和设计重点实验室，安徽 合肥　230027）

摘要：分离式霍普金森压杆(SHPB)实验常被用来获得混凝土类材料的动态压缩强度，所得数据对建立本构方程有重要作用，因此需要对其进行正确解释或分析。利用最新的混凝土材料模型研究了 SHPB 实验中试件尺寸的影响。藉由混凝土试件的体积考虑动态尺寸效应的影响，并提出了一个计算由于惯性(约束)效应引起的动态增强因子的新经验公式。结果表明：新经验公式与不同尺寸混凝土的 SHPB 模拟结果吻合得很好，且惯性(约束)效应引起的动态增强因子随着试件尺寸的增大而增大。

关键词：分离式霍普金森压杆实验；混凝土；惯性(约束)效应；试件尺寸效应；数值模拟

中图分类号：O347.3　　**文献标志码**：A